Journal of Power Sources 196 (2011) 6906–6910

Contents lists available at ScienceDirect

Journal of Power Sources

journal homepage: www.elsevier.com/locate/jpowsour

Short communication

Comparison of the surface changes on cathode during long term storage testing of high energy density cylindrical lithium-ion cells

Shoichiro Watanabe*, Masahiro Kinoshita, Kensuke Nakura

Technology Development Center, Energy Company, Panasonic Corporation, 1-1 Matsushita-cho, Moriguchi City, Osaka 570-8511, Japan

ARTICLE INFO

Article history:
Received 22 October 2010
Received in revised form 7 December 2010
Accepted 8 December 2010
Available online 21 December 2010

Keywords:
Electron energy-loss spectroscopy in a scanning transmission electron microscope
Deterioration
Storage performance
Cycle performance
Lithium nickel cobalt aluminum oxide
Lithium-ion batteries

ABSTRACT

Nickel-based oxide cathode material taking out from lithium-ion cell after storage for 2 years at 45 °C is analyzed by electron energy-loss spectroscopy in a scanning transmission electron microscope (STEM-EELS) and the result of STEM-EELS is compared with cobalt-based oxide cathode material which is treated as same manor as nickel-based oxide cathode material. The Ni-$L_{2,3}$ energy-loss near-edge structure (ELNES) spectra of nickel-based oxide cathode material show peak positions similar to original material before storage. This result indicates that nickel-based oxide material has no significant change in the surface structure. On the other hand, a remarkable shift to low energy is observed in the Co-$L_{2,3}$ ELNES spectra of the cobalt-based oxide cathode material after storage. The cycle test at 60 °C under the conditions of aggressive driving cycle (US06) mode for the nickel-based oxide cathode/graphite cell is also carried out. It is clear that cycle performance of the nickel-based oxide cathode/graphite cell is dependent on the depth of discharge (DOD).

1. Introduction

Lithium-ion batteries have been widely used for lap-top PC, cellular phones, and DSC applications because of its high energy density. While rising of environmental awareness, lithium-ion batteries are expected to be applied to high-power and electric energy storage applications. Longer calendar and cycle life are required for EV and household electric energy storage applications comparing to above conventional applications. Batteries are subjected to be stored at high state of charge (SOC), and used wide range of SOC during charge–discharge cycles for EV and household electric energy storage applications.

Panasonic launched the lithium-ion battery combined with nickel-based oxide cathode and graphite anode in 2006. This battery shows the energy density of 620 Wh dm^{-3} (18650-type 2.9 Ah cylindrical cell). Recently, Panasonic has commercialized a higher capacity of 3.1 Ah lithium-ion battery which has the high energy density of 675 Wh dm^{-3}. A battery with nickel-based oxide cathode shows much longer cycle life than a conventional battery with cobalt-based oxide cathode [1]. Crystal and electronic structures on the surface of the nickel-based oxide cathode was analyzed by XAFS and TEM-EELS [2–5] in order to investigate the capacity fade during the storage and cycle test of lithium-ion battery. In these report, it is suggested that the growth of the NiO-like rock salt structure in the surface of the nickel-based oxide cathode material causes the deterioration of lithium-ion battery with nickel-based oxide cathode.

Crystal and electronic structures of the active materials before and after storage have been investigated on this study, in order to clarify the difference of deterioration mechanism between the nickel-based oxide cathode/graphite cell and the conventional cobalt-based oxide cathode/graphite cell.

2. Experimental

The nickel-based oxide cathode/graphite cell was composed of nickel-based oxide cathode which consisted of a mixture of $LiNi_{0.8}Co_{0.15}Al_{0.05}O_2$, carbon black, poly (vinylidene fluoride) and aluminum foil, graphite anode, electrolyte and micro-porous polyethylene separator. The active material load of cathode and anode were about 20 mg cm^{-2} and 12 mg cm^{-2}, respectively. The cobalt-based oxide cathode/graphite cell was also composed of cobalt-based oxide cathode which consisted of a mixture of $LiCoO_2$, carbon black, poly(vinylidene fluoride) and aluminum foil, graphite anode, electrolyte and micro-porous polyethylene separator. The active material load of cathode and anode were about 30 mg cm^{-2} and 14 mg cm^{-2}, respectively. The electrolyte used is 1.0 M LiPF6 dissolved in ethylene carbonate (EC)/ethyl methyl carbonate (EMC)/dimethyl carbonate (DMC) (2/2/6 by volume). The surface structure of cathode materials was observed by elec-

* Corresponding author. Tel.: +81 6 6994 4630; fax: +81 6 6998 3179.
E-mail address: watanabe.sho-ichiro@jp.panasonic.com (S. Watanabe).

0378-7753/$ – see front matter © 2010 Elsevier B.V. All rights reserved.
doi:10.1016/j.jpowsour.2010.12.028

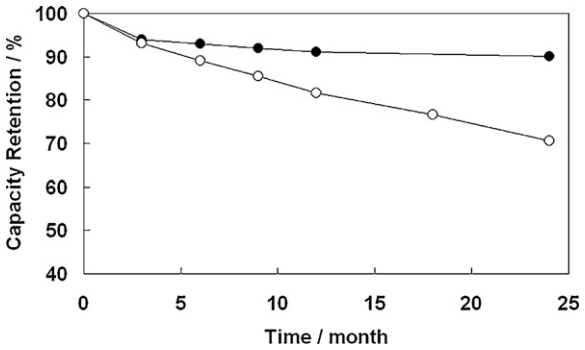

Fig. 1. Storage performances at 45 °C of the cells charged at 4.1 V. Closed and open circles indicate the nickel-based oxide cathode/graphite cell (2.9 Ah, NCR18650) and the cobalt-based oxide cathode/graphite cell (2.6 Ah, CGR18650E), respectively. The type of these batteries is 18,650 cylindrical cells. The vertical axis indicates the recovery capacity in percent with respect to the initial discharge capacity. Before storage, the initial capacity of NCR18650 and CGR18650E were evaluated at 25 °C. After the cells were charged once again, cells were stored at 45 °C. After storage, the cells were discharged at 25 °C. Subsequently, the charging and discharging tests of the cells were performed to measure the recovery capacity. NCR18650 was charged at constant current of 580 mA up to 4.1 V followed by charging at constant voltage of 4.1 V until charging current reaches below 50 mA and discharged at 580 mA to 2.5 V. CGR18650E was charged at constant current of 520 mA up to 4.1 V followed by charging at constant voltage of 4.1 V until charging current reaches below 45 mA and discharged at 520 mA to 3.0 V.

tron energy-loss spectroscopy in a scanning transmission electron microscope (STEM-EELS). STEM-EELS studies were conducted on a JEM-2100F at 200 kV equipped with a parallel electron energy loss (EEL) spectrometer (Gatan 863). Inductively coupled plasma atomic emission spectrometry (ICP-AES) measurement was performed using ICPS-7500 in order to quantify the amount of metal deposited on the surface of anode. The cell impedance was measured by a Solartron 1260/1286 frequency response analyzer system. Other experimental conditions are given in the following section.

3. Results and discussion

Fig. 1(a) shows the results of the storage test at 45 °C for nickel-based oxide cathode/graphite cell (18650-type 2.9 Ah cylindrical cell, NCR18650) and cobalt-based oxide cathode/graphite cell (2.6 Ah cylindrical cell, CGR18650E). The two cells were stored at 4.1 V charged state. NCR18650 showed superior performance to CGR18650. NCR18650 remained 90% capacity vs. initial one even after storage for 2 years at 45 °C.

Fig. 2(a) shows ac impedance spectra of NCR18650 before and after storage for 2 years at 45 °C. The cell impedance was measured at 100% SOC under 25 °C atmosphere. The ac impedance spectra of CGR18650E before and after storage for 2 years at 45 °C are also shown in Fig. 2(b). As shown in Fig. 2, the impedance of both cells was increased after storage. The impedance of CGR18650E at the low frequency range increases 1.5 times as large as that of NCR18650 after storage for 2 years at 45 °C.

The stored cell and fresh cell were disassembled and then the cathodes were taken out from both cells. A part of cathode was reassembled into 2016 coin cells with lithium metal electrode as a counter electrode and other components were taken out from stored cells except cell case. Fig. 3 shows the discharge curves of the reassembled coin cells operated at a rate of 0.4 mA cm^{-2} in voltage range of 2.5–4.3 V at 25 °C. No significant capacity fade was observed for the nickel-based oxide cathode after storage. On the other hand, 30% capacity fade was observed from the cobalt-based oxide cathode after storage. This result suggests that the difference of capacity fade of lithium ion cells during high temperature storage as shown in Fig. 1 is depended on the degradation of cathode mainly.

STEM-EELS was used to investigate the changes in the local structure and the electronic structure of active material before and after storage for 2 years at 45 °C. Fig. 4 shows the Ni-$L_{2,3}$ energy-loss near-edge structure (ELNES) spectra from the nickel-based oxide cathode material in NCR18650 before and after storage. The Ni-$L_{2,3}$ ELNES spectra were acquired in a depth range from the surface to 100 nm depth of the nickel-based oxide cathode material particle. The peak positions of the Ni-$L_{2,3}$ ELNES spectrum from the surface of NiO particle were also shown in Fig. 4. The slight peak shift at 10 nm depth from the surface was observed in the Ni-$L_{2,3}$ ELNES spectra of the nickel-based oxide cathode material after storage. The surface crystal structure up to 10 nm from surface was identified NiO-like rock salt structure by using selected area electron diffraction (SAD) analysis, as discussed by Abraham's research group [3].

The Co-$L_{2,3}$ ELNES spectra for the cobalt-based oxide cathode material in CGR18650 before and after storage were also shown in Fig. 5. The peak positions of the Co-$L_{2,3}$ ELNES spectrum from the surface of CoO particle were shown in Fig. 5. As showed in Fig. 5, a remarkable peak shift to lower energy was observed up to the depth of 100 nm in the Co-$L_{2,3}$ ELNES spectra after storage.

These results suggest that the nickel-based oxide material has no significant change in the surface crystal and electronic structures after long term storage, which may lead to the superior storage performance of NCR18650.

Fig. 6 shows the amount of metal deposition on the surface of anode before and after storage for 2 years at 45 °C. The amount of metal deposition was quantified by using ICP-AES. The amount of Ni metal dissolution from the nickel-based oxide cathode was

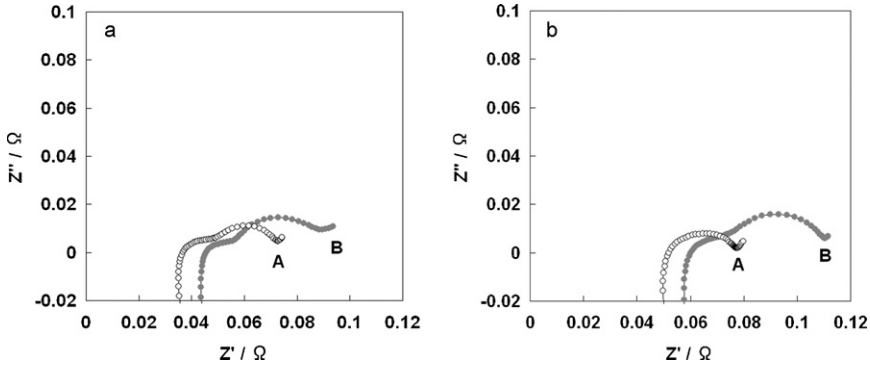

Fig. 2. Nyquist plots of the impedance spectra obtained from the charged (a) NCR18650 and (b) CGR18650E. Open and closed circles indicate the (A) fresh cell and (B) stored cell, respectively.

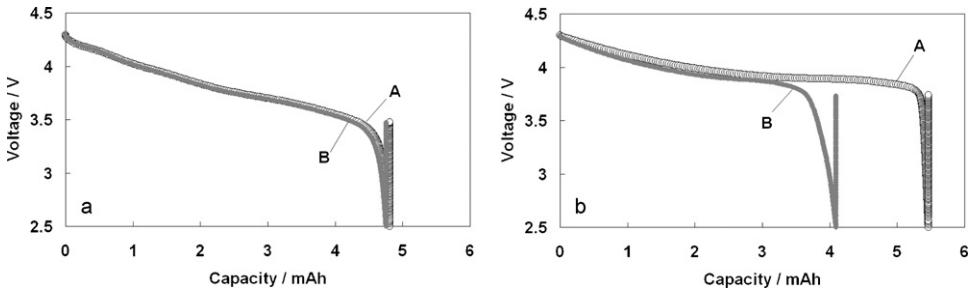

Fig. 3. Discharge curves of (a) nickel-based oxide cathode and (b) cobalt-based oxide cathode; the data of cathode obtained from the (A) fresh cell and (B) stored cell, respectively.

less than half of that of Co metal dissolution from the cobalt-based oxide cathode after storage. This result implies that the amount of Co and Ni metal dissolution from cathode material may be related to the change of surface crystal and electronic structures for the nickel-based oxide cathode and the cobalt-based oxide cathode.

The cycle performance of NCR18650 under the conditions of aggressive driving cycle (US06) mode was investigated with several depth of discharge (DOD) condition at 60 °C. As showed in Fig. 7, high retention capacity was obtained when DOD was reduced. The cycle performance became excellent when applied ranges of 0–50% DOD and 0–80% DOD. Capacity retention up to 80% DOD could achieve more than 80% at 1000 cycles.

Influence of end voltage of discharge on cycle life was investigated. Fig. 8 shows the impedance data of NCR18650 after cycling with the range of 0–50% DOD, 0–80% DOD, and fully 0–100% DOD.

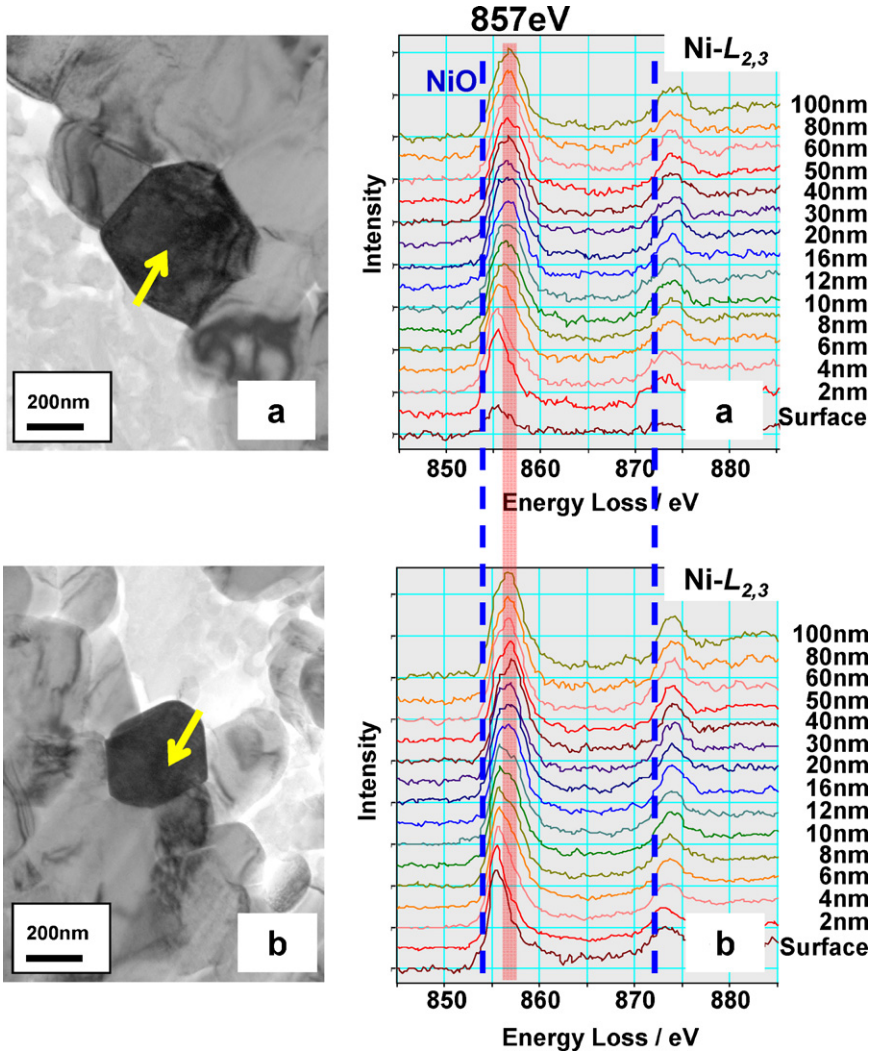

Fig. 4. Cross section TEM images and Ni-$L_{2,3}$ ELNES spectra from the nickel-based oxide cathode material taken out from the charged NCR18650: (a) fresh cathode material and (b) stored cathode material. Dash lines show the peak positions of Ni-$L_{2,3}$ ELNES spectrum from the surface of NiO particle.

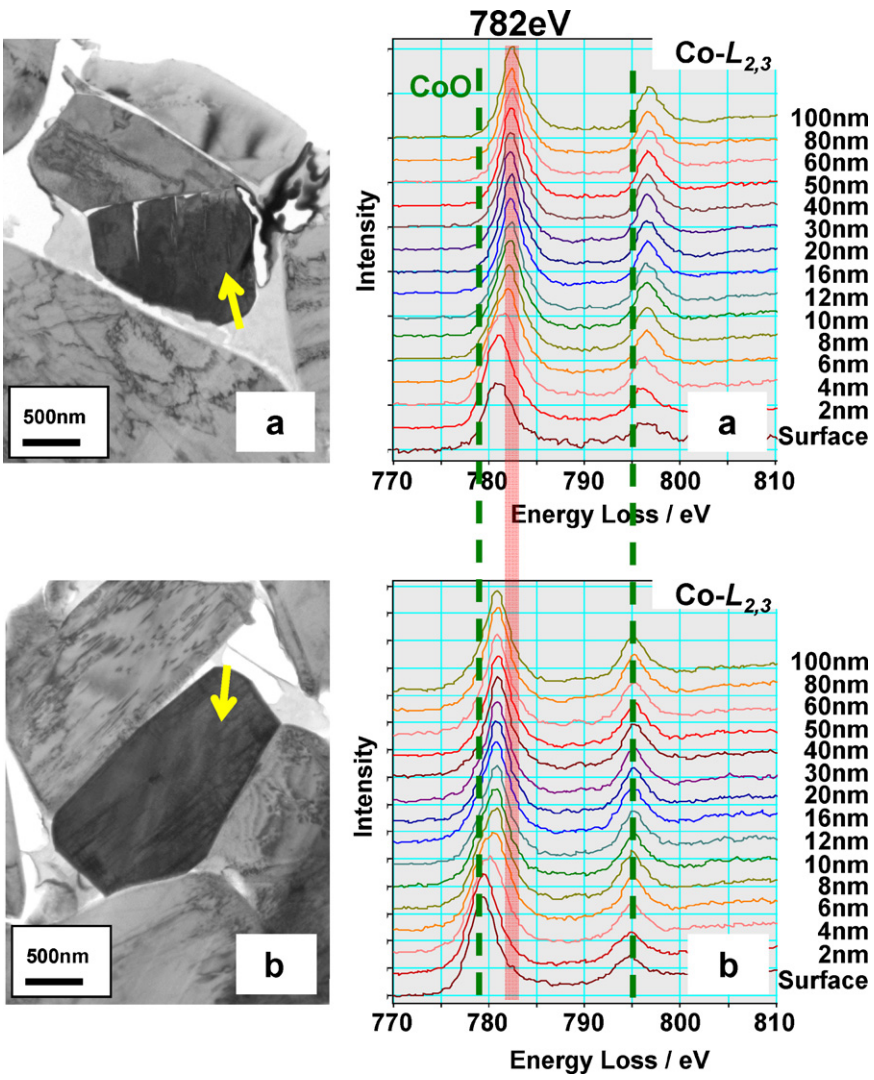

Fig. 5. Cross section TEM images and Co-$L_{2,3}$ ELNES spectra from the cobalt-based oxide cathode material taken out from the charged CGR18650E: (a) fresh cathode material and (b) stored cathode material. Dash lines show the peak positions of Co-$L_{2,3}$ ELNES spectrum from the surface of CoO particle.

When DOD range was larger, the impedance at low frequency range became higher. The cross section TEM images of the nickel-based oxide cathode particle after cycling was also shown in Fig. 8. The micro-cracks were observed in the secondary particles of the nickel-based oxide cathode material after 600 cycles with range of 0–100% DOD. This result implies that the micro-cracks of secondary particles of cathode material were highly considered as one of the causes of deterioration of cycle life.

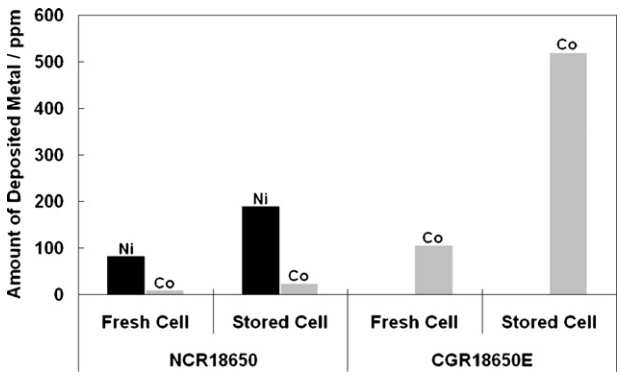

Fig. 6. Amount of metal deposition on the anode surface before and after storage for 2 years at 45 °C; deposited (■) Ni and (▒) Co.

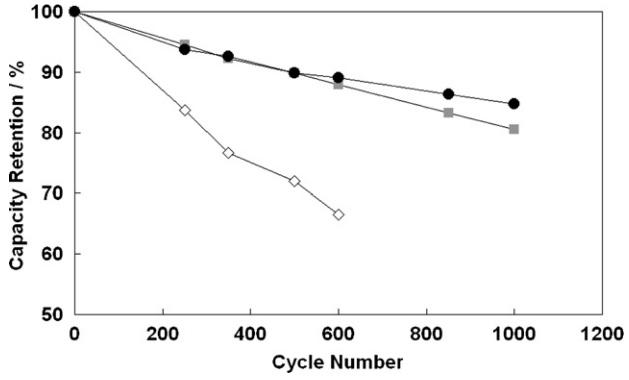

Fig. 7. Cycle performance of NCR18650 under the condition of US06 mode at 60 °C; with range of (●) 0–50% DOD, (▒) 0–80% DOD, and (◊) 0–100% DOD.

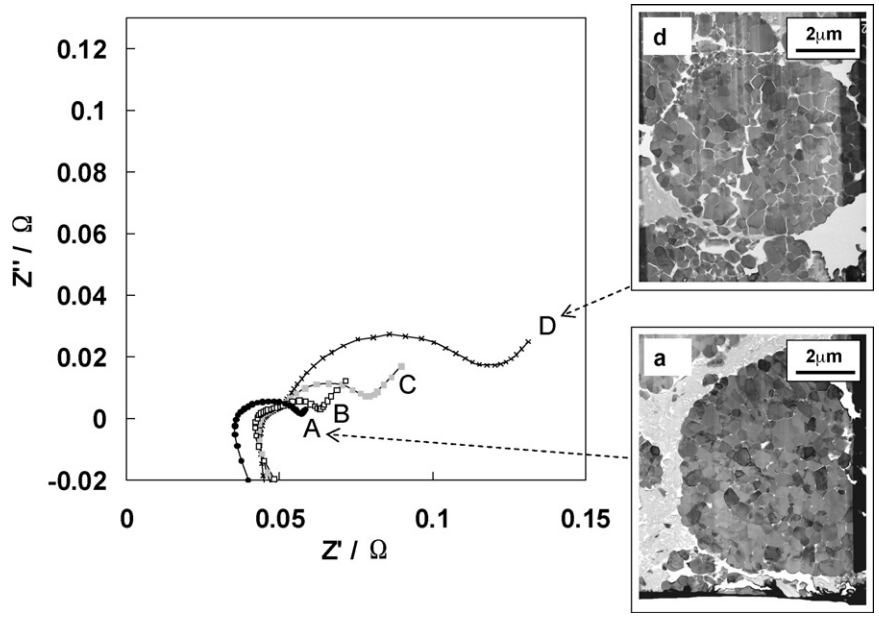

Fig. 8. Nyquist plots of the impedance spectra obtained from NCR18650: (A) before cycle, (B) after 1000 cycles with range of 0–50% DOD, (C) after 1000 cycles with range of 0–80% and (D) after 600 cycles with range of 0–100% DOD. The cross section TEM images of nickel-based oxide cathode material are also shown: (a) before cycle and (b) after 600 cycles with range of 0–100% DOD.

4. Conclusion

The nickel-based oxide cathode/graphite cell showed superior storage performance than the cobalt-based cathode/graphite cell. 90% of the initial capacity remained even after storage for 2 years at 45 °C. Comparative study using STEM-EELS of the nickel-based oxide and the cobalt-based oxide cathode material after storage verified that nickel-based oxide cathode/graphite cell has excellent storage characteristics by the observation of no significant change in the surface crystal and electronic structures of cathode material during long term storage at high temperature. Also nickel-based oxide cathode/graphite cell showed excellent cycle performance over 80% capacity at 1000 cycles at 60 °C under the condition of 0–80% DOD range. Therefore, it is suggested that the nickel-based oxide cathode/graphite cell is one of the promising lithium-ion batteries for the HEV and BEV applications.

References

[1] A. Kinoshita, K. Yanagida, A. Yanai, Y. Kida, A. Funahashi, T. Nohma, I. Yonezu, J. Power Sources 102 (2001) 283–287.
[2] S. Muto, Y. Sasano, K. Tatsumi, T. Sasaki, K. Horibuchi, Y. Takeuchi, Y. Ukyo, J. Electrochem. Soc. 156 (2009) A371.
[3] D.P. Abraham, R.D. Twesten, M. Balasubramanian, I. Petrov, J. McBreen, K. Amine, Electrochem. Commun. 4 (2002) 620.
[4] D.P. Abraham, R.D. Twesten, M. Balasubramanian, J. Kropf, D. Fischer, J. McBreen, I. Petrov, K. Amine, J. Electrochem. Soc. 150 (2003) A1450.
[5] D.Y. Itou, Y. Ukyo, J. Power Sources 146 (2005) 39.